ISBN: 978-3-95450-261-5 ISSN: 2673-7000 doi: 10.18429/JACoW-NAPAC2025-MOP073

PHYSICS CONSIDERATIONS FOR A HARP SYSTEM DESIGN AT THE SECOND TARGET STATION OF THE SPALLATION NEUTRON SOURCE *

Y. Lee†, Oak Ridge National Laboratory, Oak Ridge, TN, USA

Abstract

A harp system is being developed for monitoring proton beam profile direct upstream of the proton beam window at the Second Target Station of the Spallation Neutron Source, Oak Ridge National Laboratory. It consists of two sensor planes which have arrays of thin conducting wires aligned vertically and horizontally, respectively. It monitors beam profiles in two transverse directions to the beam axis by measuring the net-charge depositions in the sensor wires, which are caused by ejection of secondary electrons and delta rays driven by electromagnetic interactions with high-energy protons. The net charge deposition in a sensing wire linearly correlates with the number of incident protons on it. This correlation is perturbed when the wire interacts with secondary electrons and delta rays originating from beam-matter interactions in neighboring wires, PBW and residual gases. In this paper, we analyze the physical phenomena that affects the measurement uncertainties of the harp using particle transport simulations.

INTRODUCTION

The target of the Second Target Station (STS) at the Spallation Neutron Source (SNS) of the Oak Ridge National Laboratory (ORNL) will receive 1.3 GeV protons at 700 kW beam power. The beam profile on the target has a super-Gaussian shape with sharp shoulders and > 90% of the protons will hit the rectangular area spanned by $\Delta x = 128$ mm and $\Delta y = 48$ mm. The thermo-mechanical stresses in the target affecting its operability is correlated with the peak current density. As higher beam current density could cause a premature failure of the target, it is important to have a capability of monitoring the beam profile on the target during operation.

The harp wires capture beam profile measuring the charge imbalance in each conductive wire that is caused by proton induced secondary and delta-ray electron emissions. However, it does not provide information about the momentum distribution of protons when they pass through the harp wires. Therefore, it is advantageous to place the harp system as close as possible to the target as the ratio of beam footprints on the target to that on the harp is close to unity. Close to the target, there are two locations where a harp system can be installed. The first is at the target viewing periscope (TVP) end port which is 105 cm upstream from the target and the other is 20 cm upstream from the proton beam window (PBW) which is 2.6 meters upstream from the target. The TVP port is inside the target core vessel which has either a 133 Pa rough vacuum or a slightly sub-atmospheric pressure helium. The upstream region of the PBW is in accelerator vacuum at an estimated pressure of maximum $6.12 \cdot 10^{-5}$ Pa.

At the TVP end-port location, the harp signal will be disturbed by secondary and delta ray electrons from the PBW, target, neighboring wires and discharge of the core vessel gases. Also, the positive ions from gas discharge will affect the harp signal. At the PBW location, the beam current signal of a harp system will be disturbed by secondary and delta electrons from the PBW, and neighboring wires. In this paper, we study the physics that contribute to anomalous harp signal readings.

ELECTRON EMISSIONS

The net-charge deposition in a harp wire is caused by emissions of secondary and delta-ray electrons due to incident protons. The emitted secondary electrons (SE) per proton, η_{SE} is described by Sternglass theory presented in Ref. [1],

$$\eta_{\mathrm{SE}} = \frac{P \cdot \delta_s}{E_i} \frac{dE}{dz}. \tag{1}$$

Here, $P = 0.5$ is the probability of an electron escaping, $\delta_s = 1$ nm is the average depth from which the secondaries arise, and $E_i = 25$ eV is the average kinetic energy lost by the incoming particle per ionization. Finally, dE/dz is the differential proton stopping power of the wire which depend on proton energy, which can be calculated by the Bethe-Bloch formula. Tungsten and silicon carbide (SiC) are considered for wire materials. For a 1.3 GeV proton beam at STS, the calculated dE/dz for tungsten and silicon carbide is given by 22.98 MeV·cm^{-1} and 5.44 MeV·cm^{-1} respectively. The calculated SE yields per proton η_{SE} in tungsten and SiC wires are summarized in Table 1.

To calculate the delta-ray electron (DE) yields in tungsten and SiC wires, particle transport simulations have been performed for a single wire with a diameter of 0.1 mm using FLUKA [2–4]. A rectangular shaped 1.3 GeV beam with a beam footprint defined by $\Delta x = \Delta y = 0.1$ mm was used. The calculated DE yields per proton η_δ in tungsten and SiC wires are summarized in Table 1. The net-charge deposition in the tungsten wire is higher than that in the SiC wire. This indicates that the signal strength from the tungsten wires is higher than SiC for the same beam intensity. On the other hand, tungsten has higher scattering cross section than SiC for a 1.3 Gev proton, which could lead to a higher beam loss

† leey1@ornl.gov

ISBN: 978-3-95450-261-5 ISSN: 2673-7000 doi: 10.18429/JACoW-NAPAC2025-MOP073

Table 1: Electron Yields per Proton in Harp Wires

Electron Yield	Tungsten Wire	SiC Wire
η_{SE}	0.046	0.011
η_{δ}	0.043	0.027
$\eta_{SE+\delta}$	0.089	0.038

along the beam transport line from the harp to the target. Figure 1 shows the differential energy spectrum of electrons coming out from a 100 μm thin tungsten wire (left). The spectrum for a SiC wire is also similar. Note that delta-ray electrons produced are mostly in the energy range from 1 keV to 10 MeV, with a peak at $E = 1$ keV.

With the presence of gas, proton beam ionizes the gas molecules and create electron-ion pairs. The charge created from this beam-gas interaction is proportional to dose absorbed in the gas. The ratio of the dose absorbed to charge created is defined by w-value. The corresponding w-values in air and in helium are respectively given by w =32.7 [eV/e] [5] and 41.3 [eV/e] [6]. Most of the charge created are due to inelastic soft collisions of incident protons and gas molecules that excites the electron energy states and SE emissions.

For a 1.3 GeV proton, the differential energy deposition in gas are proportional to its pressure p_{gas},

$$\frac{dE}{dz} = \mathscr{E}' \cdot \frac{p_{gas}}{p_{atm}} \left[\mathrm{eV \cdot cm^{-1} \cdot proton^{-1}}\right], \qquad (2)$$

where p_{atm} is atmospheric pressure and $\mathscr{E}'$ is a gas medium dependent constant. The $\mathscr{E}'$ for air and helium are given by $2.26{\cdot}10^3$ and $3.38{\cdot}10^2$ respectively. For given differential energy deposition, the electron-ion charge production rate per unit volume during a beam pulse is calculated by

$$\dot{q} = w^{-1} \cdot \phi_p \cdot \frac{dE}{dz} \left[e \cdot \mathrm{cm^{-2} \cdot s^{-1}}\right], \qquad (3)$$

where ϕ_p is proton flux during a pulse.

To estimate the w-value of the charge creation due to inelastic hard collisions that knocks on DEs, a FLUKA simulations have been performed. A 1.3 GeV pencil beam was transported on a 10 μm thin gas target at 1 bar, which is far shorter than the stopping range of DEs with $E > 100$ eV. The calculated w-values for delta ray electron production is 7408.23 [eV/e] for air and 7314.97 [eV/e] for helium. From the w-values for the SEs and DEs, we conclude that the DEs created by the beam-gas interaction is smaller than SEs by more than two orders of magnitudes. Figure 1 shows the differential energy spectrum of electrons coming out from the 10 μm thin air target (right). The spectra for helium is similar to air. Note that delta-ray electrons produced are mostly in the energy range higher than 1 keV, with a sharp peak at $E = 1$ keV.

VOLTAGE BIASING

Consider a harp system consisting of vertical and horizontal measurement wire planes sandwiched between three

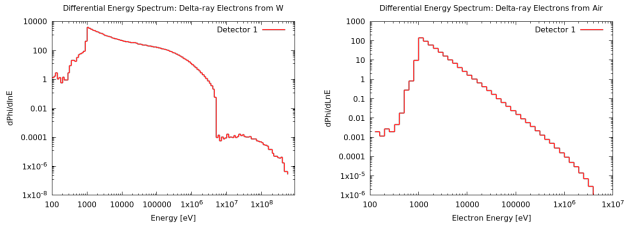

Figure 1: Differential energy spectra of delta-ray electrons coming out from coming out from a 100 μm thin tungsten wire (left) and from the 10 μm thin air target (right).

voltage biasing wire planes. The distance d between neighboring wire planes is 2 cm. The sensing wires are grounded while the biasing wires are kept at a higher voltage V_{bias}. The bias voltage shall not exceed the breakdown voltage V_B [V].

At the location of the PBW where harp is in an accelerator vacuum, the Paschen's law does not apply as there is not enough gas molecules to be ionized to cause breakdown. Extrapolation of the Paschen curves reported in Ref. [7] for $p_{air} \cdot d < 10.0$ Pa·cm indicates that the breakdown voltage is well above 1 kV by several orders of magnitudes. As such, at the PBW location, a high voltage biasing in the kV range will not cause breakdown in the harp monitor system. At a kV voltage range, a large fraction of delta-ray electrons can be captured that are originated from the sensor wires, bias wires, and PBW as Fig. 1 indicates.

In the core vessel with a rough vacuum atmosphere, the breakdown voltage in air for $p_{air} \cdot d = 2.7$ Pa·m is about 500 V. To avoid breakdown, a kV range bias voltage cannot be applied that is required to capture DEs. Consider a harp system in the core vessel filled with near atmospheric pressure helium. Extrapolating the Paschen curve based on gas parameters presented in Ref. [8] and SE emission coefficient reported in Ref. [9], the breakdown voltage in helium for $p_{helium} \cdot d = 2.0{\cdot}10^3$ Pa·m is about 100 kV. However, physical breakdown voltages in a rough vacuum and atmospheric pressure helium environment are expected to be significantly lower than the Paschen's law suggests as discussed in the following.

We consider a harp system with 500 V applied between the neighboring bias-wire and sensor-wire planes. The bias wire will capture most of the SEs with a typical kinetic energy of 25 eV. The 500 V bias is not strong enough to capture delta-ray electrons with a typical kinetic energy of 1 keV. The continuous slowing down approximation (CSDA) ranges of a 1 keV delta-ray electrons in tungsten and in SiC are less than 1 μm. Therefore, most of the DEs impinging on 100 μm thin sensor wires will be stopped in there depositing negative charges. This will disturb the harp signal based on positive charge deposition caused by electron emissions.

We consider a harp system working in helium atmosphere. The CSDA range of the positive helium ions with a kinetic energy of 1 keV in helium is given by

$$R_{CSDA:He} = 1.496 \cdot 10^{-2} \frac{p_{atm}}{p_{He}} [\mathrm{m}]. \qquad (4)$$

ISBN: 978-3-95450-261-5 ISSN: 2673-7000 doi: 10.18429/JACoW-NAPAC2025-MOP073

Simple analyses showed that the CSDA ranges are by several orders of magnitudes higher than that the ions can travel during the recombination time scale. Then, the effective ion charges per proton that are drifted towards the sensor wires can be approximately described by

$$q_{\text{ion:eff}} = w^{-1} L_{\text{eff}} \frac{dE}{dz} \quad L_{\text{eff.}} \equiv \min\left(d, R_{\text{CSDA}}\right), \qquad (5)$$

where L_{eff} is the effective distance within which the ions can reach the sensing wires. The effective charges per proton in helium is calculated to be $q_{\text{ion:eff}} = 1.22{\cdot}10^{+1}$ [$e{\cdot}\text{proton}^{-1}$]. Analyses for air at $1.33{\cdot}10^{2}$ Pa have been performed similarly and the $q_{\text{ion:eff}}$ in air is calculated to be $1.84{\cdot}10^{-1}$.

The charge deposition $q_{\text{harp:p}}$ due to emissions of SEs and DEs by proton scattering is only a small fraction of total number of protons, which is approximately given by

$$q_{\text{harp:p}} = \eta_{\text{SE+}\delta} \frac{2r}{\xi}, \qquad (6)$$

where $2r$ is the sensor wire diameter and ξ is the spacing between the wires in the same sensing plane. The wire diameter is 100 μm and the wire spacing for the x and y-wires is 6 mm and 4 mm respectively. For tungsten wires, the $q_{\text{harp:p}}$ are calculated to be $1.48{\cdot}10^{-3}$ [$e{\cdot}\text{proton}^{-1}$] and $2.23{\cdot}10^{-3}$ [$e{\cdot}\text{proton}^{-1}$] for the x and y-wires respectively. The values for the SiC wires is smaller by a factor of 2. Note that the $q_{\text{harp:p}}$ is lower than $q_{\text{ion:eff}}$ by at least two orders of magnitudes in a core vessel atmosphere. This indicates that the harp signal which is linearly correlated to proton current density is completely obscured by the positive ion capture due to voltage biasing. For this reason, voltage biasing is not recommended for a harp installed in the core vessel. In addition, the high value of $q_{\text{ion:eff}}$ in a core vessel atmosphere could cause direct current glow discharge at a much lower voltage than V_{B} discussed above. For these reasons, a harp with voltage bias planes is not advised in the core vessel.

At the potential harp locations, electron fluxes are calculated. At the PBW location, the estimated combined DE and SE flux averaged over a 240 mm × 96 mm cross section area is about $2{\cdot}10^{-5}$ [$e{\cdot}\text{cm}^{-2}{\cdot}\text{proton}^{-1}$]. This is smaller than the averaged proton flux $4{\cdot}10^{-3}$ [$\text{H}^{+}{\cdot}\text{cm}^{-2}{\cdot}\text{proton}^{-1}$] by more than two orders of magnitudes. In the presence of wire planes, the DEs from the proton-wire interaction increases the electron flux by the same number. Therefore, there is only limited benefit of having three bias wire planes. While it cleans the SE background, it contributes to production of significant background DE flux via proton-wire interactions disturbing the sensor wire signals. Furthermore, the limited functional advantage of bias planes could be significantly diminished by the increased complexity of the design. For a harp system in the core vessel environments, the combined DE and SE flux averaged over the 240 mm × 96 mm cross section area is about $4{\cdot}10^{-4}$ [$e{\cdot}\text{cm}^{-2}{\cdot}\text{proton}^{-1}$] in helium and $8{\cdot}10^{-5}$ [$e{\cdot}\text{cm}^{-2}{\cdot}\text{proton}^{-1}$] in rough vacuum. Considering that net yields of SEs and DEs in the sensing wire is less than one tenth of the protons impinging, the high electron flux could completely obscure the desired harp signal. For the reasons stated above, it is decided that a simple harp design without biasing wires will be installed at the PBW location.

SIMULATION OF HARP SIGNALS

The harp system is located at 20 cm upstream from the PBW. The PBW is a 5 mm thick plate made of Al6061-T6. Harp consists of two sensor planes separated by 4 cm. FLUKA simulations have been made to calculate the net charge deposition in the sensor wires due to DE emissions. The DELTARAY and EMFCUT cards were used with an electron transport energy threshold of 100 eV.

Figure 2 shows the calculated net charge deposition in the tungsten sensor wires due to DE emissions. Each data point shows a large statistical variations. The solid lines shown in the graphs are super-Gaussian fit of the data points. Note that the sensor wires read negative beam current in the halo region, where electron flux exceeds the proton flux. The calculated charge depositions due to DE emissions from the sensor wires showed stochastic distribution not exactly following the source beam profile. However, the peak current density obtained by Super-Gaussian function fitting of the calculated data points agreed with that of the source beam profile within 5% error.

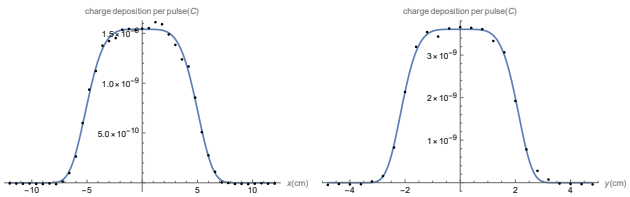

Figure 2: The calculated net charge deposition in the sensor wires (discrete symbols) and the super-Gaussian fits (solid lines) for the x (left) and y-wires (right).

CONCLUSION

A harp system will monitor the beam profile at 20 cm upstream of the PBW. The harp is in an accelerator vacuum environment. This minimizes the risks of glow discharge of residual gas molecules under voltage biasing and excessive production of SEs and DEs from the proton-gas interactions that obscure the harp signal. The harp system consists of vertical and horizontal sensor wire planes without biasing planes. While additional biasing planes can capture SEs, it cannot clean signal backgrounds from high energy DEs from neighboring wires and the PBW. As the fluxes of SEs and DEs are in the same order of magnitude, additional biasing planes will not effectively lower the backgrounds while significantly increasing the design complexity. Though the DEs affect the proton beam current reading in beam halo region, a super-Gaussian fit of the sensor wire data can be used to predict the peak current density with up to 5% error.

ISBN: 978-3-95450-261-5 ISSN: 2673-7000 doi: 10.18429/JACoW-NAPAC2025-MOP073

REFERENCES

[1] S. J. Sternglass, "Theory of secondary electron emission by high-speed ions", *Phys. Rev.*, vol. 108, no. 1, pp. 1–12, 1957. doi:10.1103/PhysRev.108.1

[2] FLUKA, https://fluka.cern

[3] G. Battistoni *et al.*, "Overview of the FLUKA code", *Ann. Nucl. Energy*, vol. 82, pp. 10–18, 2015. doi:10.1016/j.anucene.2014.11.007

[4] C. Ahdida *et al.*, "New capabilities of the FLUKA multi-Purpose code", *Front. Phys.*, vol. 9, p. 788253, 2022. doi:10.3389/fphy.2021.788253

[5] M. F. Moyers, S. M. Vatnitsky, D. W. Miller and J. M. Slater, "Determination of the air w-value in proton beams using ionization chambers with gas flow capability", *Med. Phys.*, vol. 27, no. 10, pp. 2363-2368, 2000. doi:10.1118/1.1308085

[6] R. L. Platzman, "Total ionization in gases by high-energy particles: An appraisal of our understanding", *Int. J. Appl. Radiat. Isot.*, Vol. 10, pp. 116-127, 1961. doi:10.1016/0020-708X(61)90108-9

[7] M. Klas and Š. Matejčík, "DC breakdown in air, oxygen and nitrogen at micrometer separations", in *Proc. 12th Int. Symp. High Press, Low Temp, Plasma Chem. (HAKONE)*, vol. 2, pp. 112–116, 2010.

[8] M. A. Lieberman and A. J. Lichtenberg, *Principles of plasma discharges and materials processing, 2nd Ed.*, Hoboken, NJ, USA: Wiley-Interscience, 2005. doi:10.1002/0471724254

[9] D. Marić *et al.*, "Gas breakdown and secondary electron yields," *Eur. Phys. J. D*, vol 68, p. 155, 2014. doi:10.1140/epjd/e2014-50090-x